

EIGHTH EUROPEAN ROTORCRAFT FORUM

Paper No 3.12

APPLICATION OF THE LOCAL CIRCULATION METHOD
TO THE FLUTTER ANALYSIS OF ROTARY WINGS

AKIRA AZUMA and KEIJI KAWACHI

The University of Tokyo,

TAKATOSHI HAYASHI

Nissan Automobile Company

and

AKIRA ITO

Meiji University

August 31 through September 3, 1982

AIX-EN-PROVENCE, FRANCE

APPLICATION OF THE LOCAL CIRCULATION METHOD
TO THE FLUTTER ANALYSIS OF ROTARY WINGS

by

AKIRA AZUMA and KEIJI KAWACHI
The University of Tokyo,

TAKATOSHI HAYASHI
Nissan Automobile Company

and

AKIRA ITO
Meiji University
Tokyo 153, Japan

ABSTRACT

A simple method of numerical calculation to determine the critical torsional rigidity or the classical flutter boundary of rotary wings has been proposed as an extensive work of the Local Circulation Method (LCM). Exemplified calculations were performed for a helicopter rotor and a windmill rotor. The result for the helicopter rotor shows good correlation with that of the theoretical computation based on the lifting surface theory and with the experimental test. The result for the windmill rotor, which does not have any comparable subject of reference, shows a possibility of calculation for the windmill operating in yawed condition with respect to the wind direction.

NOMENCLATURE

a nondimensional position of elastic axis based on the half chord
b half chord length = $c/2$
 $C(k)$ Theodorsen function = $F(k) + iG(k)$
 C_{My} nondimensional bending moment = $M_y / \rho S (R\Omega)^2 R$
 $C_l(\alpha)$ lift coefficient
 c^l blade chord
 $F(k)$ real part of the Theodorsen function
 $G(k)$ Imaginary part of the Theodorsen function

h normal displacement of a blade element, positive downward
 I_{θ} moment of inertia about feathering hinge
 i inclination angle of tip-path-plane with respect to the general flow
 i imaginary = $\sqrt{-1}$
 k reduced frequency at flutter $k=b\omega/U$
 k_{β} flapping stiffness about the flapping hinge
 k_{θ} feathering stiffness about the feathering hinge
 l lift acting on a blade element= l_1+l_2
 l_1 apparent mass component of the lift l
 l_2 circulatory component of the lift l
 M aerodynamic pitching moment acting on a blade
 M_y flapwise bending moment of rotor blade
 m mass of rotor blade or moment acting on a blade element= m_1+m_2
 m_1 apparent mass component of the moment m
 m_2 circulatory component of the moment m
 N normal aerodynamic force acting on a blade
 R rotor radius
 r radius position of rotor blade
 r_{β} radius position of flapping hinge
 S rotor area= πR^2
 $S(k)$ Sears function
 U stationary inflow velocity= $\sqrt{U_T^2+U_P^2}$
 U_T tangential component of the inflow velocity
 $\overline{U_T}$ stationary component of U_T
 U_P normal component of the inflow velocity
 $\overline{U_P}$ stationary component of U_P
 V wind velocity
 v^j induced velocity generated by the preceding j -th blade
 Δv induced velocity generated by the blade under consideration
 x nondimensional distance= r/R
 x_f nondimensional radius of gyration defined in equation (A.3)
 x_{β} nondimensional radius of either actual
or equivalent flapping hinge r_{β}/R
 $x_{f,a}, \overline{x_{\beta}}, \overline{x}$, nondimensional quantity defined in equation (A.3)
 y_{CG} nondimensional CG position based on the chord, positive
forward from the elastic axis
 $\overline{y_{CG}}$ nondimensional mean CG position
 α angle of attack of a blade element= $\theta-\phi$
 α_G angle of attack caused by the induced velocity= $-(\sum_j v^j + \Delta v)/U$
 β flapping angle
 β_0 coning angle
 θ feathering angle
 θ_0 initial feathering angle or pitch angle of a blade element
 μ advance ratio = $V \cos i / R\Omega$
 ρ air density

ϕ	stationary inflow angle $=\tan^{-1}(-U_P/U_T)$
Ψ	yawing angle of the rotor shaft
ψ	azimuth angle $=\Omega t$
Ω	angular velocity of rotor or rotor speed
ω	resonant frequency or flutter frequency
ω_θ	undamped natural frequency of torsion
ω_1	undamped natural frequency of the flapwise bending
ω_1^N	undamped natural frequency of the flapwise bending of non-rotating blade
$(\dot{\quad})$	time differentiation of ()

§1 INTRODUCTION

It has been paid attention to the classical flutter, coupled vibration of bending and torsional motions, of rotary wings as well as fixed wings in many years. Since the respective blade of rotary wings is operated in the field of large centrifugal force and of strong downwash left by the preceding blades, more sophisticated analysis is required than that of fixed wings.

Major differences of the dynamic characteristics of the propeller and windmill rotor from those of the helicopter rotor are as follows: (i) the inflow angle of the propeller and windmill blade is highly distorted along the blade span and requires to have large twist or washout in propeller and washin in windmill because they are principally operated in the axial flow, and (ii) the ratio of the aerodynamic force to the inertial force, typically represented by Lock number, is small.

The analysis for finding the critical speed of initiation of the blade flutter requires to know the time- and span-wise variation of the induced velocity precisely and to get the instantaneous airloading successively.

The Local Circulation Method (LCM)¹⁾ has been developed as an extension of the Local Momentum Theory (LMT)²⁾ to calculate the dynamic airloading of the blade of rotary wings in highly distorted inflow angle. Since this method of calculation is based on the instantaneous circulation distribution of the blade the unsteady phenomena can be treated easily. In this paper the flutter of helicopter rotor and windmill rotor will be analyzed by the LCM.

§2 EQUATIONS OF MOTION

The rotor blade treated here is, as shown in Fig. 1, assumed to have both flapping and feathering hinges and to be rigid other than these hinges. Thus equations of motion about these hinges can be given by

$$\left. \begin{aligned} & \int_{r_\beta}^R \left\{ (r-r_\beta)^2 \ddot{\beta} + r(r-r_\beta) \Omega^2 \beta + c y_{CG} (r-r_\beta) \ddot{\theta} + c y_{CG} r \Omega^2 \theta \right\} \left(\frac{dm}{dr} \right) dr \\ & + k_\beta (\beta - \beta_0) = \int_{r_\beta}^r (r-r_\beta) \left(\frac{dN}{dr} \right) dr \end{aligned} \right\} \quad (2.1)$$

$$\left. \begin{aligned} & \int_{r_\beta}^R \left[(\ddot{\theta} + \Omega^2 \theta) \left(\frac{dI}{dr} \right) + c y_{CG} \left\{ (r-r_\beta) \ddot{\beta} + r \Omega^2 \beta \right\} \left(\frac{dm}{dr} \right) \right] dr \\ & + k_\theta (\theta - \theta_0) = \int_{r_\beta}^R \left(\frac{dM}{dr} \right) dr. \end{aligned} \right\} \quad (2.2)$$

When the blade has no flapping hinge actually, an equivalent hinge must be introduced as stated in APPENDIX.

If the rotor is operating without stall in axial flow only and if the induced velocity is assumed uniform, then the linear perturbation equations can be deduced from the above equations and thus the critical rotational speed of flutter can be found by solving the characteristic equations of the system.³⁾

If the rotor is operating in an inclined flow, then the coefficients of the above perturbed equation are periodic functions of azimuth angle and thus the solution can be given by using the Froquet's theorem.^{4,6)}

When the effect of flow variation on the blade airloading is considered, the vortex theory is commonly used in order to estimate the change of induced velocities generated by the blade itself and the preceding blades.^{7,9)} In this case, however, the timewise trace of the blade motion is required to find whether the amplitudes of the motion for any mode are diverging or converging.^{10,12)} Since this process of computation needs lengthy time for a great many cycles of

motion if the effect of shed vortices is taken into account,^{13,14)} the reduction of computation time for one cycle of motion is desirable.

§3 LCM FOR UNSTEADY FLOW

The tangential and normal components of the inflow velocity with respect to a blade element are, as shown in Fig.1, given respectively by

$$\left. \begin{aligned} U_T &= R\Omega(x+\mu\sin\psi)\mp(\sum_j v^j + \Delta v)\sin\phi \\ U_P &= -R\Omega\mu\tan i\mp(\sum_j v^j + \Delta v)\cos\phi - \dot{\beta}(r-r_\beta) - R\Omega\beta\mu\cos\psi \end{aligned} \right\} \quad (3.1)$$

where

$$\left. \begin{aligned} \phi &= \tan^{-1}(-U_P/U_T) \\ U_P &= -R\Omega\mu\tan i \\ U_T &= R\Omega(x+\mu\sin\psi) \end{aligned} \right\} \quad (3.2)$$

and where \mp sign of the induced velocities means to take negative for helicopter rotor and positive for windmill rotor respectively.

Then the lift and moment of the blade element can be given by

$$\left. \begin{aligned} l &= l_1 + l_2 \\ m &= m_1 + m_2 \end{aligned} \right\} \quad (3.3)$$

where $()_1$ and $()_2$ show the apparent mass components and circulatory components respectively, and are, hence, given by

$$\left. \begin{aligned} l_1 &= \rho\pi b^2(\dot{h} + U\dot{\alpha} - a\ddot{\alpha}) \\ m_1 &= \rho\pi b^3\{a\dot{h} - U(\frac{1}{2} - a)\dot{\alpha} - b(\frac{1}{8} + a^2)\ddot{\alpha}\} \end{aligned} \right\} \quad (3.4)$$

$$\left. \begin{aligned} l_2 &= \rho U^2 b \{C(k)C_l(\alpha) + S(k)C_l(\alpha_g)\} \\ m_2 &= b(a + \frac{1}{2})l_2, \end{aligned} \right\} \quad (3.5)$$

and where

$$\left. \begin{aligned} U &= \sqrt{U_T^2 + U_P^2} \\ \dot{h} &= \{-(r-r_\beta)\dot{\beta} - R\Omega\beta\cos\psi\}\cos\phi \\ \alpha &= \theta - \phi = \theta - \tan^{-1}(-U_P/U_T) \\ \alpha_g &= -(\sum_j v^j + \Delta v)/U. \end{aligned} \right\} \quad (3.6)$$

The induced velocity mainly generated by the trailing vortices, $\sum_j v^j + \Delta v$, has been regarded as if there is a vertical gust for the blade element. The effect of shed vortices on the lift and moment has been represented by the Theodorsen and Sears functions. Actually, since the circulatory component l_2 consists of many harmonics each of which has the reduced frequency of k , the above circulatory components can further be divided into low and high frequency components as stated later.

The induced velocity generated by the preceding blades and left on the rotor rotational plane, $\sum_j v^j$, can be calculated by the way proposed in Ref.1 and 2. The induced velocity generated by the blade element under consideration, Δv , may be calculated by the way written in Ref.15. Here, however, the Δv is assumed to be calculated by the momentum balance in quasi-steady flow for simplification of the computation.

§4 EXAMPLES

An exemplified calculation by means of the LCM was performed for the flutter boundary of a model helicopter rotor, the dimensions and operating conditions of which are given in Table 1. The calculation was proceeded as follows : (i) After attained a trimmed state of the rotor by performing several rotations with fixed feathering axis, a step disturbance of blade pitch angle was introduced and the feathering motion was released. (ii) By watching the behaviour of the feathering and flapping motions in several rotations, the flutter boundary could be determined and the computation was stopped.

The critical values in torsional rigidity versus advance ratio of the torsion-flapping flutter is presented as shown in Fig. 2 in comparison with theoretical calculation based on the vortex theory, and with experimental tests in the wind tunnel.^{13,14)}

In the calculation by the LCM, the Theodorsen and Sears functions are assumed to be that (i) $C(k)=S(k)=1.0$ for low frequency less than the order of the rotor rotational speed Ω , and (ii) $C(k)=S(k)$ for high frequency at critical condition of flutter $\omega \gg \Omega$.

Shown by a dotted line is the flutter boundary obtained from the

quasi-steady calculation¹⁴⁾ in which the Theodorsen function was assumed to be $C(k)=1.0$. If either the torsional rigidity represented by the undamped natural frequency of the torsion ω_θ is smaller or the rotational speed Ω is larger than that specified by this line, the system will be unstable.

By considering the unsteady effect, which was obtained by multiplying the real part of the Theodorsen function into the quasi-steady lift and moment, and by introducing the blade cutoff of 3 percent radius at blade root and tip,¹³⁾ the flutter boundary shifts downward as shown by a chain line and hence the system increases the stability.

The lifting surface theory¹⁴⁾ with rigid wake shown by a double chain line gives a closer boundary with that of the experimental test,¹⁴⁾ which is given by a thin solid line with triangular marks, than other results based on the simplified vortex theory.

The present method of calculation, the LCM, gives more conservative result, as shown by a thick line, than that of the lifting surface theory. This result well coincides with the experimental result at hovering state and goes away as the advance ratio increases. The difference from either the experimental test or the lifting surface theory is, however, within allowable range in the practical application. For the study of the sensitivity of the Theodorsen function, more simplified calculations were performed by assuming that the $C(k)$ was approximated by (i) $C(k)=F(k)$ and (ii) $C(k)=1$. The results are respectively shown by (i) a hatched line for various advance ratios and (ii) a circle for hovering flight. The difference between the results of the simplified calculation (i) and of the LCM for fully unsteady flow with $C(k)$ is essentially caused by the effect of shed vortices, whereas the difference between the results of the simplified calculation (ii) and the LCM for fully unsteady flow with $C(k)$ is resulted from phase difference of the Theodorsen function. The above tendency is almost independent to the collective pitch of the rotor.

Fig.3 shows the critical torsional rigidity or flutter boundary of a windmill rotor (see Table 1) calculated by the present method , the LCM for fully unsteady flow with $C(k)$, as a function of nondimensional center of gravity,

$$\bar{y}_{CG} = \frac{\int_{r_\beta}^R cy_{CG}(r-r_\beta)(dm/dr)dr}{\int_{r_\beta}^R (r-r_\beta)^2(dm/dr)dr},$$

in comparison with a numerical result based on the blade element theory combined with the uniform inflow distribution.¹⁶⁾ It can be seen that the latter result gives very conservative boundary.

Shown in Fig.4 is an example of nondimensional bending moment at blade root of another windmill versus yawing angle of the rotor shaft with respect to the wind direction, calculated by the LCM. Since it was found that the bending moment was strongly affected by the yaw angle, the flutter analysis of the windmill was extended to the rotor in yawed state.

Fig.5 shows the effect of the yaw angle on the flutter boundary of the windmill rotor given in Table 1. As the yaw angle increases, the critical value of the torsional rigidity increases a little within the yaw angle from 0° to 30° specifically in higher wind speed.

CONCLUSION

A simple method of numerical calculation to determine the critical torsional rigidity for the initiation of classical flutter of rotory wings has been proposed as an extensive work of the Local Circulation Method, LCM. The method was initially applied to find the flutter boundary of a helicopter rotor for which the theoretical calculation based on the lifting surface theory and wind tunnel test were performed and approved to show good correlation with these results. Then, the method has been extended to analyze the flutter boundary of windmill rotor for which the inflow angle is highly distorted along the blade span. It is believed that the boundary was clearly specified more than that calculated by the blade element theory based on the simple momentum balance.

APPENDIX

By following Young's method¹⁷⁾ the equivalent stiffness and hinge offset of a flexible blade, both in nondimensional form, can be given by

$$k_{\beta}/m(R\Omega)^2 x_f^2 = (\omega_1^N/\Omega)^2 = (\omega_1/\Omega)^2 - (x_{f,a}/x_f)^2 \quad (A.1)$$

$$x_{\beta} = \bar{x}_{\beta} \left[1 - \frac{1}{2} \left(\frac{x_f}{x_{f,a}} \right) \sqrt{ \left[1 - \frac{\bar{x}_{\beta}^2}{(x_{\beta})^2} \right] \left\{ 1 - \left(\frac{x_f}{x_{f,a}} \right) \right\} + \left\{ \frac{1}{2} \left(\frac{x_f}{x_{f,a}} \right) \right\}^2 } \right] \quad (A.2)$$

$$\approx \bar{x} \left[1 - \frac{1}{2} \left(\frac{x_f}{x_{f,a}} \right) \sqrt{ \left[1 - \frac{\bar{x}^2}{(\bar{x})^2} \right] \left\{ 1 - \left(\frac{x_f}{x_{f,a}} \right) \right\} + \left\{ \frac{1}{2} \left(\frac{x_f}{x_{f,a}} \right) \right\}^2 } \right]$$

where

$$\left(\frac{x_{f,a}}{x_f} \right)^2 = 1 + x_{\beta} (\bar{x}_{\beta} - x_{\beta}) / x_f^2$$

$$x_f^2 = \int_{x_{\beta}}^1 \left(\frac{dm}{dx} / m \right) (x - x_{\beta})^2 dx \Big/ \int_{x_{\beta}}^1 \left(\frac{dm}{dx} / m \right) dx$$

$$= \bar{x}_{\beta}^2 - 2x_{\beta} \bar{x}_{\beta} + x_{\beta}^2 \quad (A.3)$$

$$\bar{x}_{\beta}^n = \int_{x_{\beta}}^1 \left(\frac{dm}{dx} / m \right) x^n dx \Big/ \int_{x_{\beta}}^1 \left(- \frac{dm}{dx} / m \right) dx ; n=1,2$$

$$\bar{x}^n = \bar{x}_{\beta}^n \quad \text{for } x_{\beta} = 0$$

and where ω_1 and ω_1^N are undamped natural frequencies of rotating and nonrotating blade respectively.

REFERENCES

1. A. Azuma, K. Nasu, and T. Hayashi : An Extension of the Local Momentum Theory to The Rotors Operating in Twisted Flow Field. Seventh European Rotorcraft and Powered Lift Aircraft Forum, 8-11 September 1981, Garmisch-Partenkirchen, Federal Republic of Germany, and will be published in Vertica.

2. A. Azuma and K. Kawachi : Local Momentum Theory and Its Application to the Rotary Wing. Journal of Aircraft, Vol. 16, No. 1, January 1979, pp. 6-14.
3. A. M. Feingold : Theory of Mechanical Oscillations of Rotors with Two Hinged Blades. NACA Wartime Report ARR No. 3113, September 1943.
4. O. J. Lewis : The Stability of Rotor Blade Flapping Motion at High Tip Speed Ratio. British A.R.C., R. & M., No. 3544, 1963.
5. D. A. Peters and K. Hohenemser : Application of the Floquet Transition Matrix to Problems of Lifting Rotor Stability. Journal of the American Helicopter Society, Vol. 16, No. 2, April, 1971, pp. 25-33.
6. P. Friedmann and C. E. Hammond : Efficient Numerical Treatment of Periodic Systems with Application to Stability Problems. International Journal for Numerical Methods in Engineering, Vol. 11, 1977, pp. 1117-1136.
7. R. Timman and A. I. van de Vooren : Flutter of Helicopter Rotor Rotating in Its Own Wake. Journal of the Aeronautical Sciences, Vol. 24, No. 9, September 1957, pp. 694-702.
8. K. W. Shipman and E. R. Wood : A Two-Dimensional Theory for Rotor Blade Flutter in Forward Flight. Journal of Aircraft, Vol. 8, No. 12, December 1971, pp. 1008-1015.
9. C. J. Astill and C. F. Niebanch : Prediction of Rotor Instability at High Forward Speeds. Vol. II, Classical Flutter. USAAVLABS TR 68-18B, February 1969, AD 683-861.
10. A. Gessow and A. D. Crim : A Method for Studying the Transient Blade-Flapping Behavior of Lifting Rotors at Extreme Operating Conditions. NACA TN 3366, January 1955.
11. J. L. Jenkins Jr. : A Numerical Method for Studying the Transient Blade Motions of a Rotor with Flapping and Lead-Lag Degrees of Freedom. NASA TN D-4195, October 1967.
12. P. Crimi : A Method for Analyzing the Aeroelastic Stability of a Helicopter Rotor in Forward Flight. NASA CR-1332, August 1969.
13. K. Kato : A Study on the Bending-Torsion Flutter of the Helicopter Rotor Blade. Doctoral Dissertation, Faculty of Eng., The University of Tokyo, Tokyo, Japan, 1972, in Japanese.

14. K. Kato : A Numerical Approach to the Unsteady Aerodynamic Forces of the Helicopter Rotor Blade. Journal of the Japan Society for Aeronautical and Space Sciences. Vol. 22, No. 247, August 1974, pp. 390~397, in Japanese.
15. A. Azuma and S. Saito : Study of Rotor Gust Response by Means of the Local Momentum Theory. Journal of the American Helicopter Society, January 1982, pp. 58~72.
16. Kaman Aerospace Corporation : Design Study of Wind Turbines 50 kW to 300 kW for Electric Utility Applications Analysis and Design. NASA CR-134937, February 1976.
17. M. I. Young : A Simplified Theory of Hingeless Rotors with Application to Tandem Helicopters. Proceedings of the Eighteenth Annual National Forum of the American Helicopter Society, May, 1962, pp. 38~45.

Table 1 Rotor parameters and operating conditions

Items	Helicopter rotor ¹³⁾	Windmill rotor ¹⁶⁾
Rotor radius, R, m	0.907	22.9
Blade chord at 0.75R, m	0.084	1.31
Blade section	0012	230XX
Blade twist from root to tip, deg.	0	-22~2(nonlinear)
Collective pitch angle at 0.75R, deg.	4.0	0.0
Number of blades	1	2
Flapping hinge offset, m	0.047	—
Position of elastic axis (from leading-edge)	0.25c	0.25c
Non-dimensional position of C.G., y_{CG}	-0.20	—
Order of reduced frequency at 0.75R	0.2	0.4
Lock number	9.4	1.4

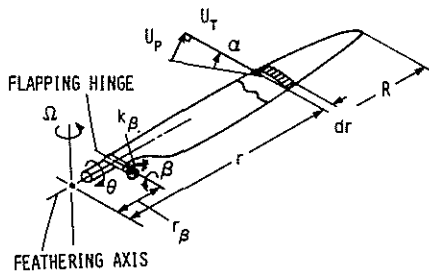


Figure 1 Blade configuration.

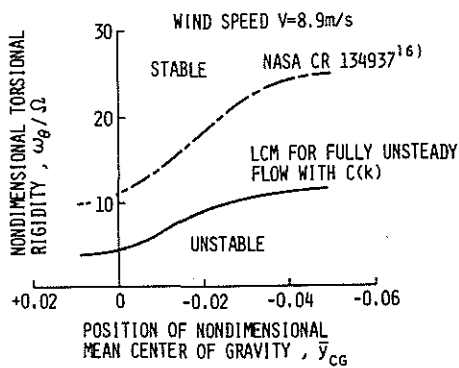


Figure 3 Flutter boundary of a windmill rotor.

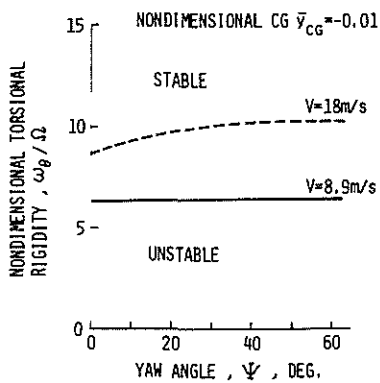


Figure 5 Flutter boundary of a windmill rotor versus yawing angle.

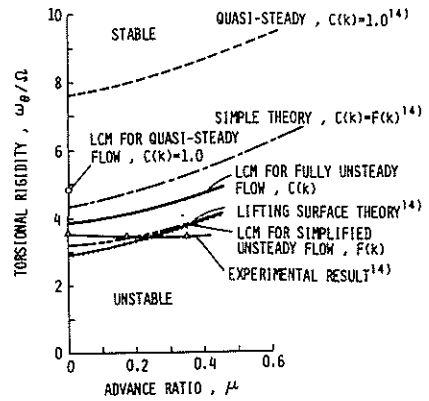


Figure 2 Flutter boundary of a helicopter rotor.

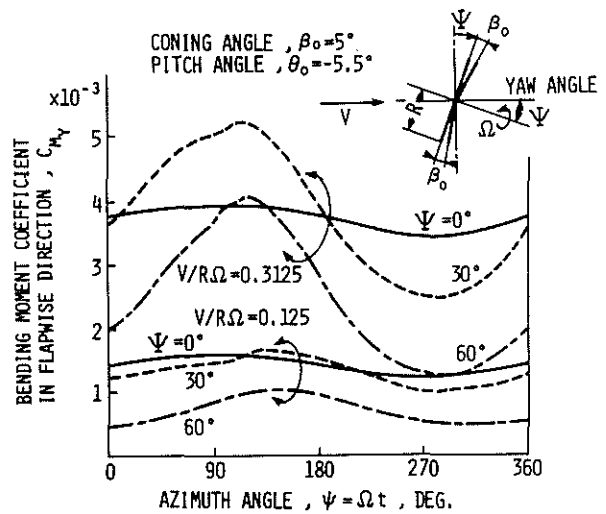


Figure 4 Variation of the bending moment of a windmill blade versus yawing angle.